Revisiting Brownian motion as a description of animal movement: a comparison to experimental movement data

Running head: Brownian motion of *Tenebrio molitor* beetles, Word count: 7000

Daniel Bearup (corresponding author)
Institute for Chemistry and Biology of the Marine Environment, University of Oldenburg,
26111 Oldenburg, Germany
email: daniel.bearup@uni-oldenburg.de
phone: +49 441 798 3612
fax: +49 441 798 3404

Carly M. Benefer
School of Biological Sciences, University of Plymouth,
Plymouth PL4 8AA, United Kingdom

Sergei V. Petrovskii
Department of Mathematics, University of Leicester,
Leicester LE1 7RH, United Kingdom

Rod P. Blackshaw
Blackshaw Research and Consulting,
Devon, TQ13 0JF, United Kingdom

doi: 10.1111/2041-210X.12615

Abstract

1. Characterisation of patterns of animal movement is a major challenge in ecology with applications to conservation, biological invasions, and pest monitoring. Brownian random walks, and diffusive flux as their mean field counterpart, provide one framework in which to consider this problem. However, it remains subject to debate and controversy. This study presents a test of the diffusion framework using movement data obtained from controlled experiments.
2. Walking beetles (*Tenebrio molitor*) were released in an open circular arena with a central hole and the number of individuals falling from the arena edges was monitored over time. These boundary counts were compared, using curve fitting, to the predictions of a diffusion model. The diffusion model is solved precisely, without using numerical simulations.
3. We find that the shape of the curves derived from the diffusion model is a close match to those found experimentally. Furthermore, in general, estimates of the total population obtained from the relevant solution of the diffusion equation are in excellent agreement with the experimental population. Estimates of the dispersal rate of individuals depend on how accurately the initial release distribution is incorporated into the model.
4. We therefore show that diffusive flux is a very good approximation to the movement of a population of *Tenebrio molitor* beetles. As such, we suggest that it is an adequate theoretical/modelling framework for ecological studies that account for insect movement, although it can be context-specific. An immediate practical application of this can be found in the interpretation of trap counts, in particular for the purpose of pest monitoring.

Keywords: random walk, trapping, population flux, diffusion, *Tenebrio molitor*

1 Introduction

Understanding of the patterns of individual animal movement and the identification of a relevant theoretical/mathematical framework to describe the corresponding dynamics of individuals and populations is a major challenge for ecology and ecological modelling (Turchin, 1998; Okubo and Levin, 2001; Lewis et al., 2013). Such a framework is required in order to enhance the predictive power of models used in population dynamics and ecology, in particular, in the context of conservation biology (Levin et al., 1984; Reichenbach et al., 2007), biological invasions (Hengeveld, 1989; Shigesada and Kawasaki, 1997; Petrovskii and Li, 2006) and pest monitoring (Petrovskii et al., 2012, 2014a,b).

Many earlier studies resulted in the conclusion that Brownian motion is an appropriate model of individual movement (Skellam, 1951; Kareiva, 1983), at least when the movement is considered at sufficiently

large temporal and spatial scales (Kareiva and Shigesada, 1983). An adequate mathematical framework to describe the spatial distribution of the corresponding population is then the diffusion equation (which turns into the diffusion-reaction equation if the events of births and deaths are taken into account). This traditional approach has been challenged over the last two decades by growing empirical evidence that, at least in some cases, animals can follow different movement patterns namely Lévy flights or walks (Viswanathan et al., 1996; Reynolds et al., 2007; Sims et al., 2008; Viswanathan et al., 2011; Reynolds et al., 2013). There is also a theoretical argument showing that Lévy-type movement can optimize search efficiency (Viswanathan et al., 2000; Bartumeus and Catalan, 2009; Mendez et al., 2014) and hence may have emerged as a result of natural selection (de Jager et al., 2011). Hence the question arises as to whether the standard diffusion equation is ecologically relevant, or whether it should be replaced altogether by a different and technically much more challenging modelling framework such as "fractional diffusion" as the mean-field counterpart of the Lévy walk (Balakrishnan, 1985; Metzler and Klafter, 2000; Sokolov and Klafter, 2002).

We note that the issue of animal movement remains controversial. There is some ambiguity as to which movement pattern animals employ and under what conditions, and what could be an efficient mathematical framework to describe it. One reason for this ambiguity is the difficulty of statistical analysis and interpretation of movement data; examples include studies of albatrosses (Viswanathan et al., 1996; Edwards et al., 2007) and mussels (de Jager et al., 2011, 2012; Jansen et al., 2012). A more fundamental reason is the inherent complexity of individual animal movement that cannot be adequately reflected by the crude dichotomy between diffusion (Brownian motion) and Lévy walks. Whilst there are theoretical arguments, and considerable empirical evidence, indicating that simple organisms like insects and other invertebrates often perform Brownian motion (Hapca at el., 2009; Jansen et al., 2012; Kareiva, 1983) (but see Reynolds et al. (2007) for an example of non-Brownian movement), more cognitively advanced animals such as mammals and reptiles may well use movement patterns that are not described by the standard diffusion process (Sims et al., 2008). Moreover, the actual movement pattern can also be context-specific, e.g. animals which perform Brownian motion in a feeding patch with abundant resources may switch to a faster 'scale-free' Lévy walk when foraging in a resource-scarce environment (Bartumeus and Catalan, 2009). The situation becomes even more complicated when the focus is scaled up from individuals to populations, as density dependence and demographic variability (individual differences) may become factors. For instance, when a population of Lévy walking organisms interact strongly, for example if their movement is stopped when they encounter each other, the otherwise fat-tailed kernels can become truncated resulting in diffusive population dispersal (de Jager et al., 2014). Conversely, fat-tailed "Lévy-like" dispersal kernels with asymptotic power law decay may also arise from pooling together movement data for a population of non-identical individuals moving diffusively (Hapca at el., 2009; Petrovskii and Morozov, 2009). However, the boundary flux of a population of Lévy walking individuals can be well described by a modified diffusion equation (Petrovskii et al.,

2014a; Ahmed and Petrovskii, 2015).

Several recent studies suggest that diffusion is an efficient theoretical framework in the context of insect pest monitoring, in particular as a tool for trap counts interpretation (Ahmed and Petrovskii, 2015; Bearup and Petrovskii, 2015; Bearup et al., 2015). However, there remain a number of open questions. One particular concern is whether a mean-field model, such as the diffusion equation, is able to provide a sensible description of the movement of a relatively small group of animals, where the variance of the stochastic fluctuations is large and the population density becomes poorly defined. This issue becomes especially relevant when monitoring low density populations, which may be required for dangerous pests. Also, it is not clear whether the intrinsically isotropic diffusion framework is able to account for the apparent anisotropy in animal movement that originates from the simple fact that every animal has a front and rear end (Pyke, 2015) which, ultimately, results in the correlated random walk rather than Brownian motion (Kareiva and Shigesada, 1983) and hence in a model different from the diffusion equation (Othmer and Xue, 2013). Although these issues have, to some extent, been addressed previously using simulated data obtained with individual based models, e.g. Petrovskii et al. (2012, 2014a), a convincing test of the theory on real movement data has been lacking so far.

In this paper, we analyse the results of a laboratory study on the walking movement of *Tenebrio molitor* beetles. Adult beetles were released in an open circular arena containing a central pitfall trap in a series of replicated experiments. This experimental setup is partially motivated by the application of the diffusion equation to model trap counts for the needs of ecological monitoring (Petrovskii et al., 2012, 2014a). In their movement, some of the beetles eventually approached the arena edge or the pitfall trap and fell over, and the number of insects that crossed the edge and the timing of the fall were recorded. The number of insects that fell over the edge is then regarded as the population flux across the arena boundary and is fitted to the corresponding solutions of the diffusion equation. We show that there is excellent agreement between the diffusion theory and the data for realistic parameter values and initial conditions.

2 Materials and methods

2.1 Experimental method

The boundary count data used in this study were obtained from controlled laboratory experiments with cultured adult *Tenebrio molitor* beetles. A novel, custom-made white plywood arena without walls (Fig. 1) was used to prevent edge following behaviour, a common phenomenon in arena studies (Creed and Miller, 1990; Valante et al., 2007). It consisted of a raised circular platform, radius $r_E = 63.25$cm, with a central hole, radius $r_I = 9.5$cm, which simulated the pitfall traps that are commonly

used to passively trap ground walking invertebrates. The beetles could fall off the arena surface from either of these edges and were subsequently collected by a moat around the edge, or a tray underneath the central hole. In order to control the release time and initial positions of the study population, individuals were placed on the surface of the arena in individual plastic tubes from which they could not escape. These tubes were connected to a PVC frame which when lifted (via the handles either side) simultaneously released all individuals. The tubes were arranged in eight concentric rings, 6cm apart, with the first ring 13.75cm from the centre of the arena. There were twelve tubes in each ring, thus the radial distance between release points in the same ring was 30°. Note that for technical reasons the full 96 release points were not used in any given run, instead four trials were combined to produce a complete time series. A video camera placed above the arena was used to monitor the insects' positions in real time, with recording starting as soon as the frame was removed. Observer XT11 (Noldus Information Technology, Netherlands) was used to analyse the footage for each experiment by recording the time at which beetles left the arena and from which edge (inner or outer). Video records of beetle movement did not reveal any changes in the movement behaviour near the edges of the arena.

The experiment was repeated four times; in the first experiment 4 rows of tubes were used in each trial, whereas in the other three experiments 3 rows were used. Summary statistics (and in particular the number of individuals released in each experiments) are shown in Table 1. Some beetles remained inside the tubes when the frame was removed and so were removed from the experiment ('Not released', Table 1), and some became upturned and could not right themselves and so were not subsequently trapped ('Not trapped', Table 1), meaning numbers released and trapped varied between experiments. Trials were ended when all beetles were trapped or the remaining beetles were upturned. The experimental data are included in Bearup et al. (2016).

The release mechanism described above attempts to simulate the uniform release of individuals within the arena, using regularly spaced release points. The reasoning behind this choice is two fold: firstly, in field applications it is generally most reasonable to assume a uniform initial population distribution; and secondly, such a distribution is relatively easy to use mathematically. While the true release distribution is more accurately characterised as a set of individual point source releases, this does not significantly impact the trap counts obtained. In particular, the initially structured distribution disappears after a short period of time due to the essentially random movement of individuals on the arena, see for example Fig. 2. A more detailed analysis of this issue can be found in Appendix A.1.

Nonetheless, there are two significant deviations from a uniform distribution which must be taken into account. Firstly, while the number of individuals at a given release distance from the trap is constant, this means that the population density declines as the radial distance over which these individuals are spread increases. In practice this means the release distribution is better described by a reciprocal distribution (i.e. density decreases as $1/r$, see Section 2.2) than a uniform distribution.

Secondly, there are gaps (of 4.25 and 7.5cm respectively) between the inner and outer edges of the domain and the innermost and outermost release points. This places a lower limit on the time it takes for the first individual to be trapped, i.e. the time required for an individual to cross one of the gap. For a truly uniform release distribution this delay does not occur, in fact the highest instantaneous trapping rate (effectively infinite) is attained at the first time point (Petrovskii et al., 2012; Bearup et al., 2015). This discrepancy can significantly impact curve fitting algorithms, so we consider the stepped forms of the initial distributions (see Section 2.2) in addition to their fundamental forms.

2.2 Modelling framework

In the experimental system described above, individuals leave the arena when they reach one or other of its boundaries. Consequently the boundary count dynamics are primarily determined by the movement pattern of individuals within the arena. While, in principle, each individual makes movement decisions in response to a variety of stimuli, in practice those stimuli can often be regarded as random (see Turchin (1998) for an enlightening discussion of this issue), so movement can be modelled as a random walk (Skellam, 1951; Turchin, 1998; Codling et al., 2008; Viswanathan et al., 2011). This simplification is especially appropriate for this experiment since the arena is devoid of stimuli except for responses to other individuals.

Reasonable boundary count time series can be obtained by simulating random walking populations directly (Petrovskii et al., 2012). However, this (fundamentally numerical) approach does not readily produce functional relationships between boundary counts and the parameters of interest, i.e. movement speed and population size. These issues can be addressed for many random walks by deriving mean field approximations; analytical expressions for the average behaviour of a population. In particular, for Brownian motion the mean field approximation of the distribution of individuals within the domain, $u(\mathbf{x})$, can be obtained by solving the diffusion equation (see Turchin (1998) for its use in an ecological context):

$$\frac{\partial u}{\partial t} = D\Delta u. \tag{1}$$

For a finite domain the flux resulting from diffusive movement through a given point, $\mathbf{x}_\gamma$, on a boundary, Γ, is then given by:

$$j(\mathbf{x}_\gamma) = D\nabla_{\hat{\mathbf{n}}} u(\mathbf{x}_\gamma), \tag{2}$$

where $\mathbf{n}$ is the outward facing unit normal vector (to the boundary). The total flux though a boundary can then be obtained by integrating along that boundary:

$$F = \int_\Gamma j(\mathbf{x}_\gamma) ds. \tag{3}$$

Finally, the fraction of the population that leaves the domain through the given boundary over a period

$t = 0$ to T, which we will call the cumulative flux, is given by:

$$N_T = \int_0^T J dt. \tag{4}$$

The cumulative flux is the mean field approximation to the cumulative count obtained at a given boundary.

The precise form of these equations depends on the domain geometry and the initial population distribution. In the special case of a circular or annular domain (such as the experimental arena) the solutions for the diffusion equation are known for many choices of initial distribution (Carslaw and Jaeger, 1959). These solutions depend on zeros of the Bessel functions which can only be found numerically, but this does not preclude their use in the analysis of boundary counts. These solutions, and the fluxes derived from them, are given for the initial population distributions considered below.

2.2.1 Circular domain

We begin by considering a circular domain, $C(r, \theta) = \{(0, 0)\} \cup (0, r_E] \times [0, 2\pi)$, with an absorbing outer boundary, $u(r_E, \theta, t) = 0,\ \forall\theta,\ t > 0$. (This is a simplified description of the experimental arena omitting the inner boundary.) If we assume further that the initial population density distribution, $u(r, 0) = u_0 f(r)$, is rotationally symmetric then we obtain the following general expression for the density distribution at time, t (Carslaw and Jaeger, 1959):

$$u(r, \theta, t) = \frac{2u_0}{r_E^2} \sum_{n=1}^{\infty} \exp\left(-\lambda_n^2 D t\right) \frac{J_0(\lambda_n r)}{J_1^2(\lambda_n r_E)} \int_0^{r_E} r f(r) J_0(r\lambda_n) dr. \tag{5}$$

The terms J_0 and J_1 denote the type one Bessel functions of orders 0 and 1 respectively, while λ_n is the n-th root of $J_0(\lambda r_E) = 0$.

Note that the integral terms:

$$I_n^c = \int_0^a r f(r) J_0(r\lambda_n) dr, \tag{6}$$

are constant with respect to r and t. This allows us to derive a general expression for the flux which applies for any choice of $f(r)$ (that is rotationally symmetric). We begin by calculating the partial derivative of Eq. 5 to r at r_E (cf. Eq. 2:

$$\left.\frac{\partial u}{\partial r}\right|_{r=r_E} = -\frac{2u_0}{r_E^2} \sum_{n=1}^{\infty} \exp\left(-\lambda_n^2 D t\right) \frac{\lambda_n I_n^c}{J_1(\lambda_n r_E)}. \tag{7}$$

We then multiply the magnitude of this derivative by the circumference of the boundary (or equivalently integrate with respect to θ, cf. Eq. 3) and the diffusion coefficient, D, to obtain the total flux through the boundary at time, t:

$$F = \frac{4\pi u_0 D}{r_E} \sum_{n=1}^{\infty} \exp\left(-\lambda_n^2 D t\right) \frac{\lambda_n I_n^c}{J_1(\lambda_n r_E)}. \tag{8}$$

Finally we integrate from $t = 0$ to T (cf. Eq. 4) to obtain the following general form for the cumulative flux at time T:

$$N_T^c = \frac{4\pi u_0}{r_E} \sum_{n=1}^{\infty} \left[1 - \exp\left(-D\lambda_n^2 T\right)\right] \frac{I_n^c}{\lambda_n J_1(\lambda_n r_E)}. \tag{9}$$

Thus, for any particular (rotationally symmetric) initial density distribution, it remains to calculate the integral terms, I_n^c, given by Eq. (6). In this work we consider three fundamental initial density distributions: the uniform distribution, $f(r) = 1$; the reciprocal distribution, $f(r) = 1/r$; and the circular distribution, $f(r) = \delta(r_R - r)$. Note that the circular distribution is the closest analogue to a point source release possible given the requirement that $f(r)$ be rotationally symmetric. Additionally we consider a variant of the uniform and reciprocal distributions, where the population density is zero in the range $r_E^* < r \leq r_E$, i.e:

$$f_{\text{stepped}}(r) = \begin{cases} f(r), & 0 \leq r \leq r_E^* \\ 0 & r_E^* < r \leq r_E \end{cases}, \forall\theta. \tag{10}$$

to better account for the experimental initial conditions used, see Section 2.1. The parameter u_0 is related to the total population of the domain, U_0, as follows:

$$u_0 = \frac{U_0}{\int_0^{2\pi} \int_0^{r_E} f(r) r dr d\theta} = \frac{U_0}{2\pi \int_0^{r_E} f(r) r dr}. \tag{11}$$

The integral terms for each of these functions can be derived from solutions found in (Carslaw and Jaeger, 1959; Gradshteyn and Ryzhik, 2015) and are given, for convenience, in Table 2.

It is intuitively clear that, since the system is finite and individuals are unable to return to the domain after being captured, all individuals in the domain will, eventually, be captured. Thus the cumulative boundary count should go to U_0 as $T \to \infty$. Applying this condition on T in Eq. (9) we find that the exponential term goes to zero leaving:

$$N_\infty^c = \frac{4\pi u_0}{r_E} \sum_{n=1}^{\infty} \frac{I_n^c}{\lambda_n J_1(\lambda_n r_E)}. \tag{12}$$

For the uniform distribution, $f(r) = 1$, this reduces to $4U_0 \sum_{n=1}^{\infty} 1/(\lambda_n r_E)^2$. We recall that the $\lambda_n r_E$'s are roots of J_0 and note that the limit of this series is known to be $1/4$ (Sneddon, 1959). Thus the boundary counts in this case go to U_0 as expected. We are not aware of explicit limits for the series obtained for the remaining four cases. However, evaluating these series numerically shows that they converge to within 1% of U_0 within one hundred terms.

2.2.2 Annular domain

The annular experimental arena can be described by the annular domain, $A(r, \theta) = [r_I, r_E] \times [0, 2\pi)$, with absorbing boundaries, $u(r, \theta, t) = 0,\ r = r_I, r_E, \forall\theta,\ t > 0$. Then, proceeding as in the previous

section, we assume a rotationally symmetric initial distribution, $f(r)$, and obtain the following solution of the diffusion equation (Carslaw and Jaeger, 1959):

$$u(r,\theta,t) = \frac{\pi^2 u_0}{2} \sum_{n=1}^{\infty} \exp\left(-D\alpha_n^2 t\right) \frac{\alpha_n^2 J_0^2(r_I\alpha_n) K_0(r\alpha_n)}{J_0^2(r_I\alpha_n) - J_0^2(r_E\alpha_n)} \int_{r_I}^{r_E} r f(r) J_0(r\lambda_n) dr. \tag{13}$$

Note that, while similar in form to Eq. (5), the integral is between r_I and r_E and the expression uses a different basis function, K_0, given by:

$$K_0(r\alpha) = J_0(r\alpha)Y_0(r_E\alpha) - J_0(r_E\alpha)Y_0(r\alpha), \tag{14}$$

where Y_0 is the type 2 Bessel function of order 0. The roots used, denoted α_n, are solutions of $K_0(\alpha r_I) = 0$ rather than J_0 as for the circular domain.

As in the previous section, we obtain the cumulative flux by calculating total flux at each of the absorbing boundaries and integrating with respect to time obtaining:

$$N_T^a = \pi^3 u_0 r \sum_{n=1}^{\infty} \left[1 - \exp\left(-D\alpha_n^2 T\right)\right] \frac{J_0^2(r_I\alpha_n) K_0'(r\alpha_n) I_n^a}{J_0^2(r_I\alpha_n) - J_0^2(r_E\alpha_n)}. \tag{15}$$

The trap counts obtained at the inner and outer boundaries can then be obtained by taking $r = r_I$ or $-r_E$ (in order to obtain the outward flux) respectively. The derivative of $K_0(r\alpha_n)$, is given by:

$$K_0'(r\alpha_n) = \alpha_n \left(J_0(r_E\alpha_n)Y_1(r\alpha_n) - J_1(r\alpha_n)Y_0(r_E\alpha_n)\right), \tag{16}$$

and the integral coefficient, I_n^a, for the initial population density distributions considered, can be found in Table 2. Note that, to account for the annular domain, the stepped versions of the initial population density distributions are modified as follows:

$$f_{\text{stepped}}(r) = \begin{cases} 0 & r_I \le r < r_I^* \\ f(r) & r_I^* \le r \le r_E^* \\ 0 & r_E^* < r \le r_E \end{cases}, \forall\theta. \tag{17}$$

Similarly the relationship between u_0 and the total population U_0, Eq. (11), is modified as follows:

$$u_0 = \frac{U_0}{\int_0^{2\pi}\int_{r_I}^{r_E} f(r) r dr d\theta} = \frac{U_0}{2\pi\int_{r_I}^{r_E} f(r) r dr}. \tag{18}$$

As for the circular domain it is clear that all individuals will eventually leave the domain. Thus the sum of the cumulative fluxes through the inner and outer boundaries, should, in the long time limit, be equal to U_0. Taking $T \to \infty$ in Eq. (15) eliminates the exponential term, but we are unaware of any analytical results stating the limits of the remaining infinite series. Again, numerical evaluation shows that they converge to within 1% of U_0 in one hundred terms.

2.3 Parameter estimation

Parameters were estimated from experimental boundary count time series using the `lsqcurvefit` tool in the MATLAB Optimisation Toolbox (MATLAB, 2013). This tool minimises the sum of the square

differences between a data set and an arbitrary function. The `nlparci` tool was then used to calculate confidence intervals for these parameter estimates (Statistics and Machine Learning Toolbox, MATLAB (2013)). The MATLAB code used is included in Bearup et al. (2016). Note that these functions make use of the `besselzero` function and `Struve01` package (Winckel, 2005; Theo2, 2012) which can be obtained from the MATLAB Central File Exchange.

3 Results

In the previous section we derived expressions for the cumulative fluxes that would arise from Brownian motion in a circular (or annular) domain. In our experimental system these fluxes correspond to the cumulative boundary counts at the inner and outer boundaries. Thus, we can determine how well the diffusion framework describes the movement behaviour of our experimental populations by comparing the theoretical fluxes to the boundary count time series obtained.

3.1 Estimating parameters from the outer boundary counts

We observe that the experimental boundary counts obtained are dominated by the contribution from the outer boundary, Table 1. This is expected since the outer boundary constitutes 87% of the total boundary length. Consequently, we begin by neglecting the trap counts from the inner boundary, thus approximating the annular arena as a circular arena. This allows us to estimate parameters using the simpler analytical solutions, see Section 2.2.1.

We estimated the dispersal rate, D, total population, U_0, and associated 95% confidence intervals from the cumulative outer boundary count series for each experiment individually using the solutions for the uniform and reciprocal distributions and their stepped versions. The results are given in Table 3 and plotted for the reciprocal distributions in Fig. 3. Plots for the uniform and stepped uniform cases can be found in Appendix A.2.

Regardless of the choice of initial distribution, the fits are a good visual match to the experimental data. However, the populations and dispersal rates estimated for the uniform initial distribution differ substantially from those obtained for the other distributions, Table 1. Additionally the associated confidence intervals for this distribution are very broad (relative to the estimated parameter value), indicating that a wide range of parameter estimates would produce similar fits. In contrast, the confidence intervals for the other distributions are narrow, indicating that the parameter estimates are meaningful.

These differences between the fits arise from the gaps between the edges of the release distribution and the edges of the domain noted in Section 2.1. For a truly uniform distribution, where the population

extended all the way to the edges of the domain, the boundary counts would increase quickly on short time scales. Since they do not, a very low dispersal rate is estimated, which in turn requires that the population be very high to obtain the observed counts. This issue does not arise when using the reciprocal distribution because, in this case, the population density at the outer boundary is relatively low which is sufficient to account for the low initial counts.

Excluding the estimates for the uniform initial distribution, the estimates of total population are quite precise and are in good agreement with the actual experimental populations. (Note that we exclude individuals which were released but not trapped in these comparisons, i.e. column "Trapped" in Table 1. Such individuals were typically immobile throughout the experiment and thus unavailable for trapping.) The estimates for the reciprocal and stepped uniform initial distributions produce similar average relative errors ($|\text{Trapped} - U_0|/\text{Trapped}$) of 6% while the stepped reciprocal initial distribution performs worst with an average relative error of 15%. The estimates for this distribution perform much better when compared to the trap counts obtained at the outer boundary, producing an average relative error of 5%, while the other distributions produce average relative errors of 9%.

Recall that the data used for parameter estimation are the outer boundary counts. It then follows that the initial distribution which most accurately captures the experimental distribution, i.e. the stepped reciprocal distribution, would provide the most accurate estimates. That the other distributions produce more accurate estimates of the total population is an artifact, arising from the fact that the outer boundary counts are only a subset of the total boundary count.

Note that the population estimates are relatively consistent for all solutions, except that obtained using the uniform initial distribution. The dispersal rates differ more significantly, around 50%, between the reciprocal and stepped uniform initial distributions and the stepped reciprocal distribution. An initial analysis of dispersal rates of individuals within the same arena yielded a median rate of 9.36 $\text{cm}^2\text{min}^{-1}$ with upper and lower quartiles of 19.09 $\text{cm}^2\text{min}^{-1}$ and 7.13 $\text{cm}^2\text{min}^{-1}$ respectively (unpublished data, C.M. Benefer *et al.*). Estimates using the stepped uniform distribution are either within, or close to the upper edge, of this range, while those obtained using the other two distributions are generally higher, but still of the right order of magnitude.

3.2 Estimating parameters from the complete boundary count series

In the previous section, we estimated the dispersal rate, D, and total population, U_0, from the outer boundary counts and used the analytical solutions for a circular domain. However, while the analytical solutions for this case are simpler, it is also practical to perform parameter estimation using the solutions for an annular domain, see Section 2.2.2. We note first that the ratios between the inner and outer boundary counts differ from the ratios predicted by the analytical solutions as follows. Whereas in

the experiment the inner boundary counts contribute between 10 and 20% of the total, the analytical solutions predict that it should contribute between 25 and 35%. Because of this discrepancy, attempts to fit the cumulative fluxes to the inner and outer boundary counts simultaneously yield results that are not a particularly good match to the data, see Figs A.4 and A.5 in Appendix A.2. Instead, we estimate parameters for each boundary count series (inner or outer) and associated 95% confidence intervals separately using the corresponding annular cumulative flux (obtained by taking $r = r_I$ or $-r_E$ respectively in Eq. (15) and compare the results (Table 4). Plots for the reciprocal initial distributions are in Fig. 4 while plots for the uniform initial distributions are in Appendix A.2 (Fig. A.3).

Again regardless of the choice of initial distribution, the fits are a good visual match to the experimental data. Population estimates from the outer boundary using the uniform initial condition remain too high. In addition the same issue is observed for the reciprocal initial distribution at the inner boundary for Experiment 1, 3, and 4. This is a consequence of the relatively high population density which occurs at the inner boundary under the reciprocal initial condition. By contrast, the estimates at the inner boundary for the uniform initial distribution are relatively reasonable as the smaller trap circumference acts as a moderating factor. Estimates obtained from solutions using the two stepped distributions do not display these issues.

We observe that these population estimates are less accurate than those obtained in the previous section, with average relative errors of ≈45% for the inner boundaries and 20% or 30% for the outer boundaries. The means of these two estimates are consistently within 20% of the actual value. In addition, the dispersal rates estimated from the counts at each boundary appear to differ in a systematic way. In particular, excluding Experiment 2 which always produces a relatively high dispersal rate at the inner boundary, the dispersal rates at the inner boundary appear to be much lower than those obtained at the outer boundary. The estimates from the outer boundary all lie within the interquartile range obtained independently, with estimates using the stepped uniform distribution lying very close to the median value (unpublished data, C.M. Benefer *et al.*). However, we note that the confidence intervals associated with all estimates from the inner boundary counts are relatively broad. Only the outer boundary counts produce reasonably precise estimates.

3.3 Comparison of boundary counts arising from different movement patterns

We have shown above that the boundary flux resulting from movement of Tenebrio beetles in the experimental arena is well described by relevant solutions of the diffusion equation for realistic parameter values. However, a question now arises as to whether a similarly good description may be obtained by using a different framework, in particular a framework that would correspond to a different movement

pattern. As was discussed in the introduction, there is growing evidence that, at least under certain conditions, animals of various species employ a movement pattern that is better described by "superdiffusive" Lévy flights (or Lévy walks) than by ordinary diffusion. Therefore, one can also ask whether the diffusion framework may still be valid, at least to some extent, if the individual animal movement is non-Brownian. In this section, we will address these questions by comparing the population fluxes through the boundary that would be obtained from beetles performing a Lévy-type movement to those obtained from diffusive movement (Brownian motion).

Note that the mean field equation describing the evolution of the population density of Lévy-walking individuals is much more complicated (Balakrishnan, 1985; Metzler and Klafter, 2000; Sokolov and Klafter, 2002) and its relevant analytical solutions are not available. While the equation can be solved numerically, this also imposes considerable technical difficulties (Sousa, 2009). We therefore calculate population fluxes using the individual based modelling (IBM) approach for parameter values relevant to the experimental setup. The formulation of IBMs for movement models is well described in the literature (e.g. see (Benhamou, 2007; Jopp and Reuter, 2005; Reynolds, 2009; Petrovskii et al., 2014a)); we present the specifics of our implementation in Appendix A.3, the MATLAB code is included in Bearup et al. (2016).

In order to sensibly compare the boundary counts resulting from different movement models (as given by pdfs (A.2) and (A.3)), we must ensure that they have equivalent characteristic displacement. One standard way to do this is to equate the variance of the pdfs to obtain a relationship between the other parameters. However, this ceases to work when the range of models includes Lévy walks which do not have a finite variance. Therefore, following (Rodrigues et al., 2015) (for a more general discussion of this approach see also Section 3a in (Kawai and Petrovskii, 2012)), we instead establish this equivalence by equating survival probabilities, i.e. the probability to remain in a given area over a given time interval.

To determine the appropriate area and time to use in this equivalence relation, we note that, in our experiments, the number of beetles leaving the arena though the external boundary in the first minute is consistently about 10% of the total, cf. panels 1, 3 & 4 in Fig. 3. Since there is no evidence for density dependence in our movement data, this suggests that the probability that an individual beetle remains in the arena, i.e. its total movement in each dimension is less that r_E, in the first minute is approximately 0.9. Thus, for Brownian motion, pdf (A.2), we obtain:

$$\int_{-r_E}^{r_E} \varrho_N(\xi) d\xi \;=\; \mathrm{erf}\left(\frac{r_E}{\sqrt{2\sigma^2}}\right) \;=\; 0.9, \tag{19}$$

where erf is the error function.

In order to establish the equivalence, we require our Lévy walks satisfy the same criterion (19), that is for pdf (A.3):

$$\int_{-r_E}^{r_E} \varrho_P(\xi) d\xi \;=\; 1 - \frac{k^{\gamma-1}}{(k+r_E)^{\gamma-1}} \;=\; 0.9. \tag{20}$$

We now solve Eqs (19) & (20) for r_E and equate the results, since r_E (i.e. the arena size) is the same in both expressions. Solving the resulting equation for k we obtain:

$$k \approx \frac{1.16\sqrt{2\sigma^2}}{\left(10^{1/(\gamma-1)}-1\right)}, \tag{21}$$

having taken $\text{erf}^{-1}(0.9) \approx 1.16$.

We plot simulated boundary counts for different values of γ (see Appendix A.3 for details) in Fig. 5. It is readily seen that random walks with a small exponent ($\gamma \leq 2$) considerably overestimate the actual boundary count on short time scales, i.e. the first 20 minutes. In particular, the counts obtained for $\gamma = 2$ (red curve in Fig. 5) are larger by at least a factor of two. Note that the case $\gamma = 2$ is often regarded as a paradigm of the Lévy-type movement; with both empirical evidence (Sims et al., 2008; Viswanathan et al., 2011) and theoretical arguments (Bartumeus and Catalan, 2009; de Jager et al., 2011; Viswanathan et al., 2011) suggesting that power laws of this type are, and should be, found in nature. However, it is clearly inappropriate for describing the movement of *Tenebrio* beetles in our experimental arena.

Decreasing γ further causes the disagreement to become even more obvious. The boundary counts obtained for $\gamma = 1.35$ (magenta curve in Fig. 5) overestimate the actual count by a factor of three on short time scales. This value of γ was suggested in a study by Reynolds et al. (2013) based on the results of another experiment on *Tenebrio* beetle movement data. We will discuss possible reasons for this disagreement in the next section.

For values of γ greater than two, the differences between boundary counts coming from Lévy-type or Brownian movement becomes less drastic. In particular, for $2.5 \leq \gamma \leq 3$ the counts are very close to those obtained from Brownian motion; see the green and blue curves in Fig. 5. Interestingly, this suggests that, in the context of boundary counts and the corresponding survival probabilities, the difference between diffusive and non-diffusive movement may become somewhat superficial; they can all be described well using diffusion fluxes. This is in good agreement with some other recent results (Ahmed and Petrovskii, 2015; Petrovskii et al., 2014a).

4 Discussion

Patterns of animal movement have been an issue of much debate and controversy recently. Whether animals move in a predominantly diffusive manner (e.g. according to the pattern called the Brownian motion) or they perform a "super-diffusive" motion (e.g. Lévy walk or Lévy flight) is thought to have important implications (Codling et al., 2008; Viswanathan et al., 2011; Mendez et al., 2014; Lewis et al., 2016). In this study, our aim was to reveal the movement pattern of *Tenebrio molitor* beetles in an

experimental arena. Having analysed the data on the number of beetles crossing the inner and outer edges of the arena, we consistently observe that the cumulative population fluxes predicted by diffusion theory are a good approximation to the boundary count time series obtained in the experiment.

Our findings have a variety of theoretical and practical applications, in particular, in the context of nature conservation programmes. Indeed, having calculated the population fluxes (e.g. by using the technique that we used in this paper), one can readily estimate the fraction of a given population that leaves a certain designated area over a given time, which can be a useful measure helping to optimize the design of nature protection areas. A more realistic model of conservation areas should also take into account the complexity of ecological borders (Fagan et al., 1999) as well as the animal behaviours resulting in territoriality (Potts and Lewis, 2014); however, the identification of diffusion as an appropriate modelling framework seems to be an important result.

One immediate practical application of our results is to pest insect monitoring, in particular, to the interpretation of trap counts. While trapping is an essential tool in pest insect management, it is largely used heuristically due to the lack of a consistent theoretical/mathematical framework allowing population abundance to be calculated from trap counts. The argument made is that larger trap counts indicate a higher pest abundance, and thus that the relative size of trap counts indicate relative risk from pests. However, this does not always work because of the so called "activity-density paradigm" (Mitchell, 1963; Thiele, 1977; Thomas et al., 1998): the same trap count can appear from a large population of slowly moving insects or from a small population of fast moving insects. Recent theoretical studies have shown that separation of the effects of density from the effects of movement, and hence good absolute estimates of the population abundance, can be obtained from curve fitting using solutions of the diffusion equation (Petrovskii et al., 2012, 2014a). This is possible because the population fluxes respond differently to the population density (u_0) and to the activity as quantified by the diffusion coefficient D. (This is readily seen from Eqs. (9) and (15); while u_0 enters the right-hand side of the equations just as a coefficient, the dependence on D is more complicated.) However, those studies used simulated trap counts obtained from an individual based model. The study that we report here is the first time the technique has been tested with experimental data.

In the context of trap count interpretation, the results we obtain are quite promising in that our estimates of the released population are generally in good agreement with the known populations (cf. U_0 in Tables 3 and 4 with the values shown in the column "Trapped" in Table 1). Moreover, the parameter values estimated from the data are, for the most part, realistic for appropriate initial conditions. Only when populations become very small (cf. the inner boundary counts for Experiment 2, see Table 1) do these estimates become unreasonable; we attribute this to the effects of stochasticity. As such, the diffusion framework appears to be relatively robust to stochastic fluctuations, at least, for populations which are not very small (i.e.for the conditions of our experiment, larger than five trapped individuals). We

note though that, for the inner boundary counts, the confidence intervals surrounding our estimates are relatively broad, indicating that more data would be required to make precise estimates from these counts. We observe that varying the modelled release distribution affects our estimates of the dispersal rate (i.e. activity) rather than population (cf. Tables 3 and 4). As such, we suggest that our technique allows the effects of population density and activity to be separated. Furthermore, population estimates obtained in this way should prove robust under field conditions, where the actual distribution of individuals may be not known *a priori*.

Considering the issue of population activity in more detail, we notice that the estimated dispersal rates appear to differ systematically, dependent on which boundary is considered. In most cases, the dispersal rates obtained at the inner boundary are lower than those obtained at the outer boundary. In addition, we recall that the inner boundary counts contribute a smaller fraction of the total boundary count than is predicted by the diffusion model (cf. Section 3.2 and Figs A.4 and A.5 in Appendix A.2). In combination these two observations suggest that there is some difference, either in the trapping process or individual behaviour, between the two boundaries. However, it is hard to see any credible explanation for this. Instead, we conclude that, for a given 'best-fit' value of diffusivity D, the diffusive flux slightly under-estimates the actual boundary count at the external boundary and over-estimates it at the internal boundary. This may appear as a result of deviations in the beetles' real movement from idealized Brownian motion. This is because, in the strict sense, Brownian motion assumes that the roving 'particle' changes its direction of movement constantly (Gardiner, 1985). However, a real beetle is more likely to change its movement velocity only occasionally, e.g. as a response to its internal states or some external cues (Petrovskii et al., 2011; Tilles and Petrovskii, 2015). Thus, on a very short time-scale, its movement path is close to a straight line. A beetle starting its movement in the vicinity of a concave boundary would then be more likely to cross it than in the case of a convex boundary, because the range of movement angles which encounter the boundary would be smaller in the latter case (see Fig. 6).

Our results suggest that, on the spatial and temporal scales of our experiment, the laboratory population of *Tenebrio molitor* beetles follow a diffusive rather than superdiffusive movement pattern, because a hypothetical population of Lévy-moving beetles would produce much higher boundary counts (see Fig. 5). At first glance, this conclusion appears to disagree with another recent study on *Tenebrio molitor* movement which finds a power law step length distribution with $\gamma = 4/3$ (Reynolds et al., 2013). However, we note that Reynolds et al. (2013) define the step length distribution over a variable time interval, based on the turning points of the individual movement tracks. This variable time interval, in conjunction with their observation that the movement of these beetles is significantly autocorrelated on short time scales (up to 10 seconds), appears to be responsible for the Lévy-like step length distribution.

As such, the disagreement between our results and those of Reynolds et al. (2013) may be an artifact arising from a difference in the time scales on which each study focuses. In particular, Reynolds et al.

(2013) characterise the ballistic phase of movement that can be observed on short time scales in correlated random walks (CRW). Indeed, most of their movement data spans a 2-3 minute interval. In contrast, in our study we focus on longer term behaviour, on the time scale of 10 to 10^2 minutes, where the CRW is expected to converge to Brownian motion (Kareiva and Shigesada, 1983). As Reynolds et al. (2013) claim that their movement data are well described by a relevant solution of the Langevin equation with δ-correlated noise, it seems the most natural reconciliation of the two studies is in terms of the correlated random walk (rather than the Lévy walk), since a well-established theory predicts that, in the course of time, the corresponding solutions of the Langevin equation converge to Brownian motion, e.g. see (Tilles and Petrovskii, 2016).

We also mention that Reynolds et al. (2013) considered only two possibilities when fitting the step length distributions, i.e. the exponential distribution and the power law. Since it is well known that a mixture of a few exponentials can provide a description of movement data which is superior to the power law (Jansen et al., 2012), this is clearly insufficient. Note that movement described by such a mixture of exponentials is diffusive (Brownian motion) and not of Lévy type.

We want to emphasize that the interpretation and analysis of movement data is often challenging and controversial. As another example, in a laboratory study by Ueno et al. (2012) on walking behaviour of *Drosophila melanogaster*, it was concluded that "the hypothesis of the power-law distribution for activity bouts was not supported as compared to the exponential distribution". In a recent paper by Reynolds et al. (2015), however, it was claimed that the walking behaviour of *Drosophila melanogaster* is better described by a power law, although no clear evidence for this was provided. Such differences might be reconciled by the observation that the individual movement traits within a cohort of apparently identical invertebrates can differ by an order of magnitude or even more (Hapca at el., 2009; Petrovskii et al., 2011). Moreover, there is evidence that, within the same population, individuals sometimes display an array of movement modes, ultimately ranging from subdiffusive to superdiffusive (Sims et al., 2008). Consequently, it is possible that the overall behaviour of the population is best described by a diffusive model while specific individuals may display Lévy walk behaviour.

Our study leaves a few open questions. Firstly, the slight deviation of the data from the diffusion model that we discussed above may indicate that the Telegrapher's equations (e.g. see Codling et al. (2008); Othmer and Xue (2013)) could possibly provide an even better fit to the data as it takes into account ballistic movement on short time-scales. However, solving the Telegrapher's equations in a two-dimensional domain is technically much more challenging. Secondly, although we did not find any significant density dependence in the movement of the beetles[1], a more careful investigation of this issue might be required as this is known to be a factor that can significantly affect the movement pattern

[1] Visual analysis of the movement data revealed that the beetles sometimes moved in small groups of 2-3 animals but that was the only inter-individual interaction that we could detect.

(de Jager et al., 2014). Thirdly, we note that the arena used in our experiments is relatively small and, as such, may restrict the movement patterns that can be studied[2]. In particular, large displacements (a characteristic of Lévy flights/walks) will usually result in the individual performing them to hit the boundary. The ongoing impact of such steps, i.e. the ability to explore a large area, may therefore be lost. Whether the population fluxes may be better described by Lévy walks rather than Brownian motion if the movement is considered in a larger arena remains an open question. This remaining uncertainty can be resolved in a larger-scale experiment, either in a laboratory or a microcosm, which should become a focus of future research.

Acknowledgements

This study was partially funded by the Leverhulme Trust (grant number F/00-568/X). The authors are grateful to Johan van de Koppel and two anonymous reviewers for their helpful remarks on this manuscript.

Data Accessibility

Experimental data and MATLAB code deposited in the Dryad repository: http://datadryad.org/resource/doi:10.5061/dryad.52mb6

References

Ahmed, D.A. & Petrovskii, S.V. (2015) Time dependent diffusion as a mean field counterpart of Lévy type random walk. *Mathematical Modelling of Natural Phenomena*, 10(2), 5-26. doi: 10.1501/mmnp/201410202

Balakrishnan, V. (1985) Anomalous diffusion in one dimension. *Physica A*, 132, 569-580. doi: 10.1016/0378-4371(85)90027-7

Bartumeus, F. & Catalan, J. (2009) Optimal search behavior and classic foraging theory. *Journal of Physics A: Mathematical and Theoretical*, 42, 434002. doi: 10.1088/1751-8113/42/43/434002

Bearup, D. & Petrovskii, S.V. (2015) On time scale invariance of random walks in confined space. *Journal of Theoretical Biology*, 367, 230-245. doi: 10.1016/j.jtbi.2014.11.027

[2]We mention here that the arena size (1.2 meter) used in our experiments is consistent with the arena size (1.8 meter) used by Reynolds et al. (2013).

Bearup, D., Petrovskaya, N. & Petrovskii, S.V. (2015) Some analytical and numerical approaches to understanding trap counts resulting from pest insect immigration. *Mathematical Biosciences*, 263, 143-160. doi: 10.1016/j.mbs.2015.02.008

Bearup, D., Benefer, C.M., Petrovskii, S.V. & Blackshaw, R.P. (2016) Data from: Revisiting Brownian motion as a description of animal movement: a comparison to experimental movement data. *Methods in Ecology and Evolution*, doi: 10.5061/dryad.52mb6

Benhamou, S. (2007) How many animals really do the Lévy walk? *Ecology*, 88, 1962-1969. doi: 10.1890/06-1769.1

Carslaw, H.S. & Jaeger, J.C. (1959) *Conduction of heat in solids*, 1st edn. Clarendon Press, Oxford.

Codling, E.A., Plank, M.J. & Benhamou, S. (2008) Random walk models in biology. *Journal of the Royal Society Interface*, 5, 813-834. doi: 10.1098/rsif.2008.0014

Creed Jr R.P. & Miller, J.R. (1990) Interpreting animal wall-following behaviour. *Experientia*, 46(7), 758-761. doi: 10.1007/bf01939959

de Jager, M., Weissing, F.J., Herman, P.M.J., Nolet, B.A. & van de Koppel, J. (2011) Lévy walks evolve through interaction between movement and environmental complexity. *Science*, 332, 1551-1553. doi: 10.1126/science.1201187

de Jager, M., Weissing, F.J., Herman, P.M.J., Nolet, B.A. & van de Koppel, J. (2012) Response to comment on "Lévy walks evolve through interaction between movement and environmental complexity". Science 335, 918-d.

de Jager, M., Bartumeus, F., Kolzsch, A., Weissing, F.J., Hengeveld, G.M., Nolet, B.A., Herman, P.M.J. & van de Koppel, J. (2014) How superdiffusion gets arrested: ecological encounters explain shift from Lévy to Brownian movement. *Proceedings of the Royal Society B*, 281, 20132605. doi: 10.1098/rspb.2013.2605

Edwards, A.M., Phillips, R.A., Watkins, N.W., Freeman, M.P., Murphy, E.J., Afanasyev, V., Buldyrev, S.V., da Luz, M.G.E., Raposo, E.P., Stanley, H.E. & Viswanathan, G.M. (2007) Revisiting Lévy flight search patterns of wandering albatrosses, bumblebees and deer. *Nature*, 449, 1044-1048. doi: 10.1039/nature06199

Fagan, W.F., Cantrell, R.S. & Cosner, C. (1999) How habitat edges change species interactions. *The American Naturalist*, 153, 165-182. doi: 10.1086/303162

Gardiner, C.W. (1985). *Handbook of stochastic methods*, Volume 13 of Springer Series in Synergetics. Springer, Berlin.

Gradshteyn, I.S. & Ryzhik, I.M. (2015) *Table of integrals, series, and products*, 8th edn. Elsevier, London.

Hapca, S., Crawford, J.W. & Young, I.M. (2009) Anomalous diffusion of heterogeneous populations characterized by normal diffusion at the individual level. *Journal of the Royal Society Interface*, 6, 111-122. doi: 10.1098/rsif.2008.0261

Heinsalu, E., Hernandez-García, E., Lopez, C. (2010) Spatial clustering of interacting bugs: Lévy flights versus Gaussian jumps. *Europhysics Letters*, 92, 40011. doi: 10.1209/0295-5075/95/69902

Hengeveld, R. (1989) *Dynamics of biological invasions*. Chapman and Hall, London.

Jansen, V.A.A., Mashanova, A. & Petrovskii, S.V. (2012) Model selection and animal movement: Comment on "Lévy walks evolve through interaction between movement and environmental complexity". *Science*, 335, 918-c. doi: 10.1126/science.1215747

Jopp, F., Reuter, H. (2005) Dispersal of carabid beetles – emergence of distribution patterns. *Ecological Modelling*, 186:389-405. doi: 10.1016/j.ecolmodel.2005.02.009

Kareiva, P.M. (1983) Local movement in herbivorous insecta: applying a passive diffusion model to mark-recapture field experiments. *Oecologia*, 57, 322-327. doi: 10.1007/bf0037175

Kareiva, P.M. & Shigesada, N. (1983) Analyzing insect movement as a correlated random walk. *Oecologia*, 56, 234-238. doi: 10.1007/bf00379695

Kawai, R., Petrovskii, S.V. (2012) Multi-scale properties of random walk models of animal movement: lessons from statistical inference. *Proceedings of the Royal Society A*, 468, 1428-1451. doi: 10.1098/rspa.2011.0665

Levin, S.A., Cohen, D. & Hastings, A. (1984) Dispersal strategies in patchy environments. *Theoretical Population Biology*, 26, 165-180. doi: 10.1016/0040-5809(84)90028-5

Lewis, M.A., Maini, P.K. & Petrovskii, S.V. (eds) (2013) *Dispersal, individual movement and spatial ecology*. Springer, Berlin. doi: 10.1007/978-3-642-35497-7

Lewis, M.A., Petrovskii, S.V. & Potts, J. (2016) *The mathematics behind biological invasions*. Springer, Berlin (to appear).

MATLAB Release (2013b), The MathWorks, Inc., Natick, MA.

Mendez, V., Campos, D. & Bartumeus, F. (2014) *Stochastic foundations in movement ecology: anomalous diffusion, front propagation and random searches*. Springer, Berlin.

Metzler, R. & Klafter, J. (2000) The random walk's guide to anomalous diffusion: a fractional dynamics approach. *Physics Reports*, 339, 1-77. doi: 10.1201/b16008-9

Mitchell, B. (1963) Ecology of two carabid beetles, *Bembidion lampros* (Herbst) and *Trechus quadristriatus* (Schrank). II. Studies on populations of adults in the field, with special reference to the technique of pitfall trapping. *Journal of Animal Ecology*, 32(3), 377-392. doi: 10.2307/2599

Okubo, A. & Levin, S.A. (eds) (2001) *Diffusion and ecological problems: modern perspectives*. Springer-Verlag Inc., New York. doi: 10.1007/978-1-4757-4978-6

Othmer, H.G. & Xue, C. (2013) The mathematical analysis of biological aggregation and dispersal: progress, problems and perspectives. *Dispersal, individual movement and spatial ecology* (eds. M.A. Lewis, P.K. Maini & S.V. Petrovskii), pp. 79-128. Springer, Berlin.

Pearson, K. (1900) X. On the criterion that a given system of deviations from the probable in the case of a correlated system of variables is such that it can be reasonably supposed to have arisen from random sampling. *Philosophy Magazine Series 5*, 50(302), 157-175. doi: 10.1080/14786440009463897

Petrovskii, S.V. & Li, B.L. (2006) *Exactly solvable models of biological invasion*. CRC Press, Boca Raton.

Petrovskii, S.V. & Morozov, A.Y. (2009) Dispersal in a statistically structured population: Fat tails revisited. *The American Naturalist*, 173, 278-289. doi: 10.1086/595755

Petrovskii, S.V., Bearup, D., Ahmed, D.A. & Blackshaw, R. (2012) Estimating insect population density from trap counts. *Ecological Complexity*, 10, 69-82. doi: 10.1016/j.ecocom.2011.10.002

Petrovskii, S.V., Mashanova, A. & Jansen, V.A.A. (2011) Variation in individual walking behavior creates the impression of a Lévy flight. *Proceedings of the National Academy of Sciences of the United States of America*, 108, 8704-8707. doi: 10.1073/pnas.1015208108

Petrovskii, S.V., Petrovskaya, N. & Bearup, D. (2014) Multiscale approach to pest insect monitoring: Random walks, pattern formation, synchronization, and networks. *Physics of Life Reviews*, 11, 467-525. doi: 10.1016/j.plrev.2014.02.001

Petrovskii, S.V., Petrovskaya, N. & Bearup, D. (2014) Multiscale ecology of agroecosystems is an emerging research field that can provide a stronger theoretical background for the integrated pest management. *Physics of Life Reviews*, 11, 536-539. doi: 10.1016/j.plrev.2014.07.001

Potts, J.R. & Lewis, M.A. (2014) How do animal territories form and change? Lessons from 20 years of mechanistic modeling. *Proceedings of the Royal Society B*, 281, 20140231. doi: 10.1098/rspb.2014.0231

Pyke, G.H. (2015) Understanding movements of organisms: it's time to abandon the Lévy foraging hypothesis. *Methods in Ecology and Evolution*, 6, 1-16. doi: 10.1111/2041-210x.12298

Reichenbach, T., Mobilia, M., Frey, E. (2007) Mobility promotes and jeopardizes biodiversity in rock-paper-scissors games. *Nature*, 448, 1046-1049. doi: 10.1038/nature06095

Reynolds, A.M. (2009) Scale-free animal movement patterns: Lévy walks outperform fractional Brownian motions and fractional Lévy motions in random search scenarios. *J*ournal of Physics A: Mathematical and Theoretical 42, 434006. doi: 10.1088/1751-8113/42/43/434006

Reynolds, A.M., Smith, A.D., Menzel, R., Greggers, U., Reynolds, D.R. & Riley, J.R. (2007) Displaced honey bees perform optimal scale-free search flights. *Ecology*, 88, 1955-1961. doi: 10.1890/06-1916.1

Reynolds, A.M., Lepretre, L., Bohan, D.A. (2013) Movement patterns of Tenebrio beetles demostrate emprircally that correlated-random-walk have simultitude with a Lévy walk. *Scientific Reports*, 3, 3158. doi: 10.1038/srep03158

Reynolds, A.M., Jones, H.B.C., Hill, J.K., Pearson, A.J., Wilson, K., Wolf, S., Lim, K.S., Reynolds, D.R., Chapman, J.W. (2015) Evidence for a pervasive 'idling-mode' activity template in flying and pedestrian insects. *Royal Society Open Science*, 2, 150085. doi: 10.1098/rsos.150085

Rodrigues, L.A.D., Mistro, D.C., Cara, E.R., Petrovskaya, N., Petrovskii, S.V. (2015) Patchy invasion of stage-structured alien species with short-distance and long-distance dispersal. *Bulletin of Mathematical Biology*, 77, 1583-1619. doi: 10.1007/s11538-015-0097-1

Shigesada, N. & Kawasaki, N. (1997) *Biological invasions: theory and practice*. Oxford University Press, Oxford.

Sims, D.W., Southall, E.J., Humphries, N.E., Hays, G.C., Bradshaw, C.J.A., Pitchford, J.W., James, A., Ahmed, M.Z., Brierly, A.S., Hindell, M.A., Morritt, D., Musyl, M.K., Righton, D., Shepard, E.L.C., Wearmouth, V.J., Wilson, R.P., Witt, M.J. & Metcalfe, J.D. (2008) Scaling laws of marine predator search behaviour. *Nature*, 451, 1098-1102. doi: 10.1038/nature06518

Skellam, J.G. (1951) Random dispersal in theoretical populations. *Biometrika*, 38, 196-218. doi: 10.2307/2332328

Sneddon, I.N. (1960) On some infinite series involving the zeros of Bessel functions of the first kind. In: *Proceedings of the Glasgow Mathematical Association*, 4(3), 144-156. Cambridge University Press, Cambridge. doi: 10.1017/s2040618500034067

Sokolov, I.M., Klafter, J., Blumen, A. (2002) Fractional kinetics. Physics Today, November 2002, 48-54.

Sousa, E. (2009) Finite difference approximations for a fractional advection diffusion problem. *Journal of Computational Physics*, 228, 40384054. doi: 10.1016/j.jcp.2009.02.011

Theo2 (2012) Struve functions (http://uk.mathworks.com/fileexchange/37302-struve-functions), MATLAB Central File Exchange.

Thiele, H.U. (1977) *Carabid beetles in their environments. A study on habitat selection by adaptation in physiology and behaviour*. Springer-Verlag, Berlin.

Thomas, C.F.G., Parkinson, L. & Marshall, E.J.P. (1998) Isolating the components of activity-density for the carabid beetle Pterostichus melanarius in farmland. *Oecologia*, 116, 103-112. doi: 10.1007/s004420050568

Tilles, P.F.C. & Petrovskii, S.V. (2015) Statistical mechanics of animal movement: animal's decision-making can result in superdiffusive spread. *Ecological Complexity*, 22, 86-92. doi: 10.1016/j.ecocom.2015.02.006

Tilles, P.F.C. & Petrovskii, S.V. (2016) How animals move along? Exactly solvable model of superdiffusive spread resulting from animal's decision making. *Journal of Mathematical Biology*, in press. doi: 10.1007/s00285-015-0947-3

Ueno, T., Masuda, N., Kume, S., Kume, K. (2012) Dopamine modulates the rest period length without perturbation of its power law distribution in Drosophila melanogaster. *PLoS ONE* 7, e32007. doi: 10.1371/journal.pone.0032007

Turchin, P. (1998) *Quantitative analysis of movement: measuring and modeling population redistribution in animals and plants*. Sinauer Associates, Inc., Sunderland, MA.

Valente, D., Golani, I. & Mitra, P.P. (2007) Analysis of the trajectory of *Drosophila melanogaster* in a circular open field arena. *PLoS ONE*, 2(10), e1083. doi: 10.1371/journal.pone.0001083

Viswanathan, G.M., Afanasyev, V., Buldyrev, S.V., Murphy, E.J., Prince, P.A. & Stanley HE (1996) Lévy flight search patterns of wandering albatrosses. *Nature*, 381, 413-415. doi: 10.3410/f.1098667.554787

Viswanathan, G., Afanasyev, V., Buldryrev, S., Havlin, S., da Luz, M.G.E., Raposo, E.P. & Stanley HE (2000) Lévy flights in random searches. *Physica A*, 282, 1-12. doi: 10.1016/s0378-4371(00)00071-6

Viswanathan, G.M., da Luz, M.G.E., Raposo, E.P. & Stanley, H.E. (2011) *The physics of foraging: an introduction to random searches and biological encounters*. Cambridge University Press, Cambridge.

von Winckel, G. (2005) Bessel Function Zeros (http://uk.mathworks.com/fileexchange/6794-bessel-function-zeros), MATLAB Central File Exchange.

Table 1: Summary statistics for the four experiments. Data for each of the four trials in each experiment have been combined. Columns indicate: the number of individuals originally positioned in tubes; the number of individuals released from the tubes into the arena; the total number of individuals captured; the number of individuals trapped in the inner pitfall; the number of individuals captured at the outer edge; the number of individuals that remained in the tubes when the frame was removed; the number of individuals that became upturned and were not subsequently captured; and the average duration for all individuals to be captured.

Exp	Indiv	Released	Captured	Inner	Outer	Not released	Not trapped	Av duration/hh:mm:ss
1	128	92	84	9	75	36	8	01:18:13
2	96	52	46	4	42	44	6	00:52:43
3	96	53	47	8	39	43	6	00:55:28
4	96	56	49	10	39	40	7	01:16:14
Total	416	253	226	31	195	163	27	01:05:40*

*Average duration

Table 2: Table of integral terms, I_n^c or I_n^a, for the initial density distributions used in this work(Carslaw and Jaeger, 1959; Gradshteyn and Ryzhik, 2015). The terms $\mathbf{H}_0$, $\mathbf{H}_1$, and G denote the Struve functions of orders 0 and 1 and the Meijer G-function, $G_{33}^{11}\left(\begin{smallmatrix}1 & 1/2\\ 1,1 & 1/2,0\end{smallmatrix}\,\middle|\, x^2\right)$, respectively. All other functions are defined in the text. For brevity, the values at which functions are evaluated have been omitted for the stepped reciprocal distribution. For the circular domain all functions are evaluated at $\lambda_n r_E^*$. For the annular domain the additional subscripts I and E denote that the functions were evaluated at $\alpha_n r_I^*$ and $\alpha_n r_E^*$ respectively.

initial distribution	circular domain, I_n^c	annular domain, I_n^a
uniform	$r_E J_1(\lambda_n r_E) \,/\, \lambda_n$	$(J_0(\alpha_n r_I) - J_0(\alpha_n r_E)) \,/\, J_0(\alpha_n r_I)$
stepped uniform	$r_E^* J_1(\lambda_n r_E^*) \,/\, \lambda_n$	$1/\alpha_n \left[Y_0(\alpha_n r_E)\left(J_1(\alpha_n r_E^*) - J_1(\alpha_n r_I^*)\right) - 2J_0(\alpha_n r_E)/\alpha_n \left(G(\alpha_n r_E^*/2) - G(\alpha_n r_I^*/2)\right)\right]$
reciprocal	$\pi r_E/2\ \mathbf{H}_0(\lambda_n r_E) J_1(\lambda_n r_E)$	$\pi/2\alpha_n \left(r_I \mathbf{H}_0(\alpha_n r_I) K_0'(\alpha_n r_I) - r_E \mathbf{H}_0(\alpha_n r_E) K_0'(\alpha_n r_E)\right)$
stepped reciprocal	$r_E^* \left[J_0 + \pi/2 \left(\mathbf{H}_0 J_1 - \mathbf{H}_1 J_0\right)\right]$	$\left[r_E^* K_{0,E} - r_I^* K_{0,I} + \pi r_I^*/2 \left(\mathbf{H}_{0,I} K_{0,I}'/\alpha_n + \mathbf{H}_{1,I} K_{0,I}\right) - \pi r_E^*/2 \left(\mathbf{H}_{0,E} K_{0,E}'/\alpha_n + \mathbf{H}_{1,E} K_{0,E}\right)\right]$
circular distribution	$r_R J_0(\lambda_n r_R)$	$r_R K_0(\alpha_n r_R)$

Table 3: Parameters estimated from the experimental cumulative outer boundary count series using the analytical solutions for a circular domain (Eq. 9). The experiment number is indicated in the first column. The dispersal rate, D, total population, U_0, and associated 95% confidence intervals were estimated for the uniform and reciprocal distributions and their stepped versions. The domain geometry was chosen so that it corresponded to the experimental arena, i.e. $r_E = 63.25$cm and $r_E^* = 55.75$cm.

	Uniform			Reciprocal		
Exp	D (cm^{2}min^{-1})		U_0 (indiv)	D (cm^{2}min^{-1})		U_0 (indiv)
1	0.111	$\pm$0.085	786$\pm$314	21.4	$\pm$1.0	81$\pm$2
2	0.042	$\pm$0.043	789$\pm$445	29.0	$\pm$4.0	42$\pm$3
3	0.034	$\pm$0.026	785$\pm$338	16.7	$\pm$3.4	47$\pm$5
4	0.220	$\pm$0.247	281$\pm$161	20.4	$\pm$3.3	42$\pm$3
	Stepped uniform			Stepped reciprocal		
Exp	D (cm^{2}min^{-1})		U_0 (indiv)	D (cm^{2}min^{-1})		U_0 (indiv)
1	18.1	$\pm$1.6	82$\pm$3	29.1	$\pm$2.0	78$\pm$3
2	21.3	$\pm$2.4	46$\pm$2	37.1	$\pm$2.3	40$\pm$1
3	15.9	$\pm$3.2	45$\pm$5	25.9	$\pm$4.3	40$\pm$3
4	19.8	$\pm$3.5	40$\pm$3	31.6	$\pm$5.2	36$\pm$3

Table 4: Parameters estimated from the experimental cumulative boundary count series using the analytical solutions for an annular domain (Eq. 15). Experiment number is indicated in the first column. The dispersal rate, D, total population, U_0, and associated 95% confidence intervals were estimated from the inner and outer boundary count series separately for the uniform and reciprocal distributions and their stepped versions. The final column contains the mean of the two population estimates. The domain geometry was chosen so that it corresponded to the experimental arena, i.e. $r_I = 9.5$cm, $r_E = 63.25$cm, $r_I^* = 13.75$cm, and $r_E^* = 55.75$cm respectively.

Uniform	Inner			Outer			
Exp	D (cm^{2}min^{-1})		U_0 (indiv)	D (cm^{2}min^{-1})		U_0 (indiv)	$\overline{U_0}$ (indiv)
1	1.53	±4.96	99±196	0.0862	±0.0503	821±247	460
2	41.7	±78.0	15±7	0.0376	±0.0385	762±426	389
3	5.93	±74.8	51±389	0.0276	±0.0211	793±336	422
4	3.95	±34.7	78±426	0.133	±0.1040	336±131	207
Reciprocal	Inner			Outer			
Exp	D (cm^{2}min^{-1})		U_0 (indiv)	D (cm^{2}min^{-1})		U_0 (indiv)	$\overline{U_0}$ (indiv)
1	0.023	±0.059	320±430	7.69	±0.85	130±7	225
2	8.83	±81.1	13±42	10.4	±2.72	68±8	41
3	0.005	±0.009	1000±1420	6.09	±2.53	76±16	538
4	0.006	±0.020	1000±2210	6.43	±1.59	72±9	536
Stepped u	Inner			Outer			
Exp	D (cm^{2}min^{-1})		U_0 (indiv)	D (cm^{2}min^{-1})		U_0 (indiv)	$\overline{U_0}$ (indiv)
1	8.3	±5.89	34±11	11.2	±0.93	106±4	70
2	48.8	±76.4	12±6	13.8	±0.91	58±2	35
3	5.2	±9.3	54±74	10.4	±1.83	57±5	56
4	5.23	±11.1	63±99	12.4	±2.14	52±4	58
Stepped r	Inner			Outer			
Exp	D (cm^{2}min^{-1})		U_0 (indiv)	D (cm^{2}min^{-1})		U_0 (indiv)	$\overline{U_0}$ (indiv)
1	5.29	±5.14	31±15	13.8	±1.10	113±4	72
2	34.3	±68.0	10±5	17.3	±1.02	62±2	36
3	2.17	±2.26	64±49	12.7	±2.18	61±5	63
4	4.44	±9.35	46±59	15.2	±2.59	56±4	51

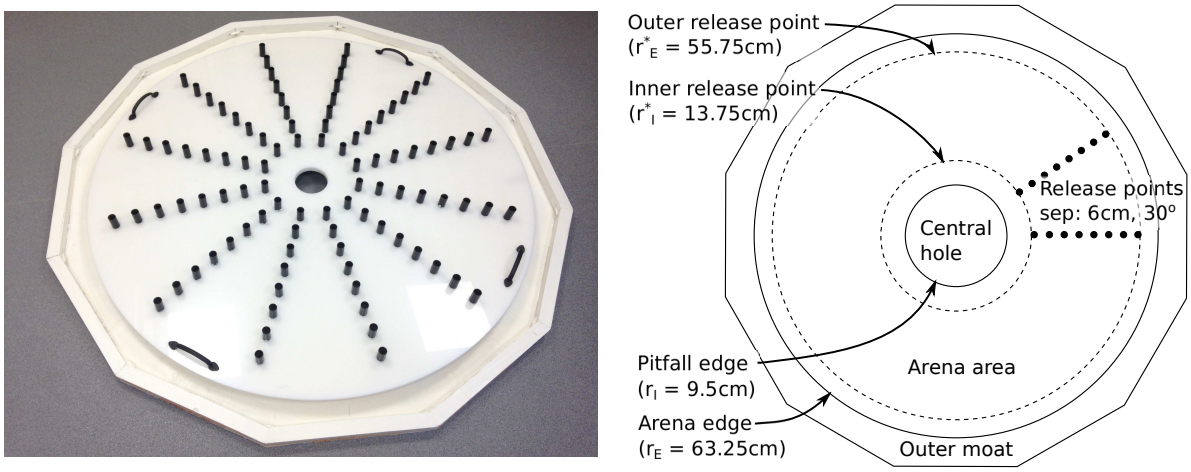

Figure 1: Experimental setup. Left: Photograph of arena and release apparatus. Right: Schematic representation of the arena (not to scale). For simplicity only two rows of release points are shown.

Figure 2: Distribution of individuals over the first ten minutes of a trial. Left: release distribution; middle: after five minutes; right: after ten minutes.

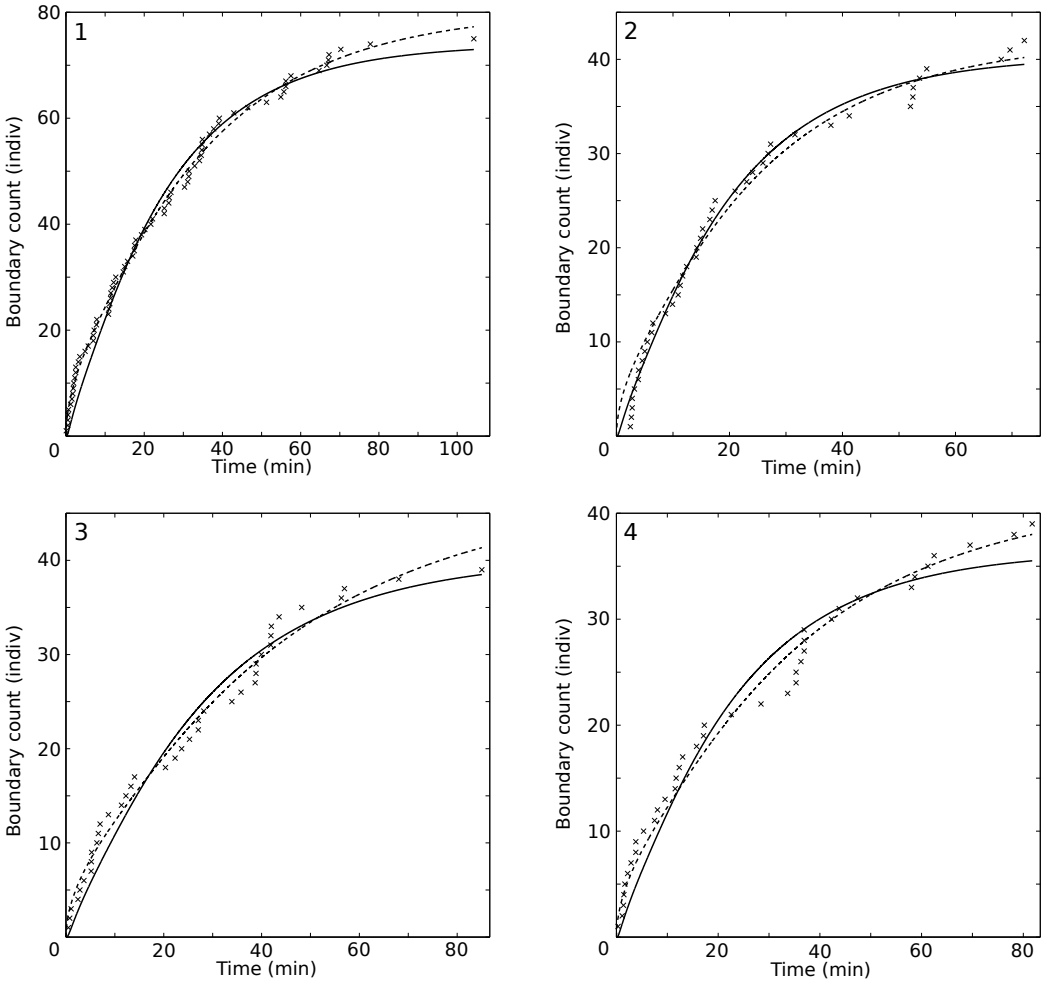

Figure 3: Plots of experimental cumulative outer boundary count series and fitted curves (using Eq. 9). The number in the top left of each plot indicates the experiment number. Crosses - experimental data, dashed and solid curves - fits using the solution for a reciprocal or stepped reciprocal initial distribution in a circular domain respectively.

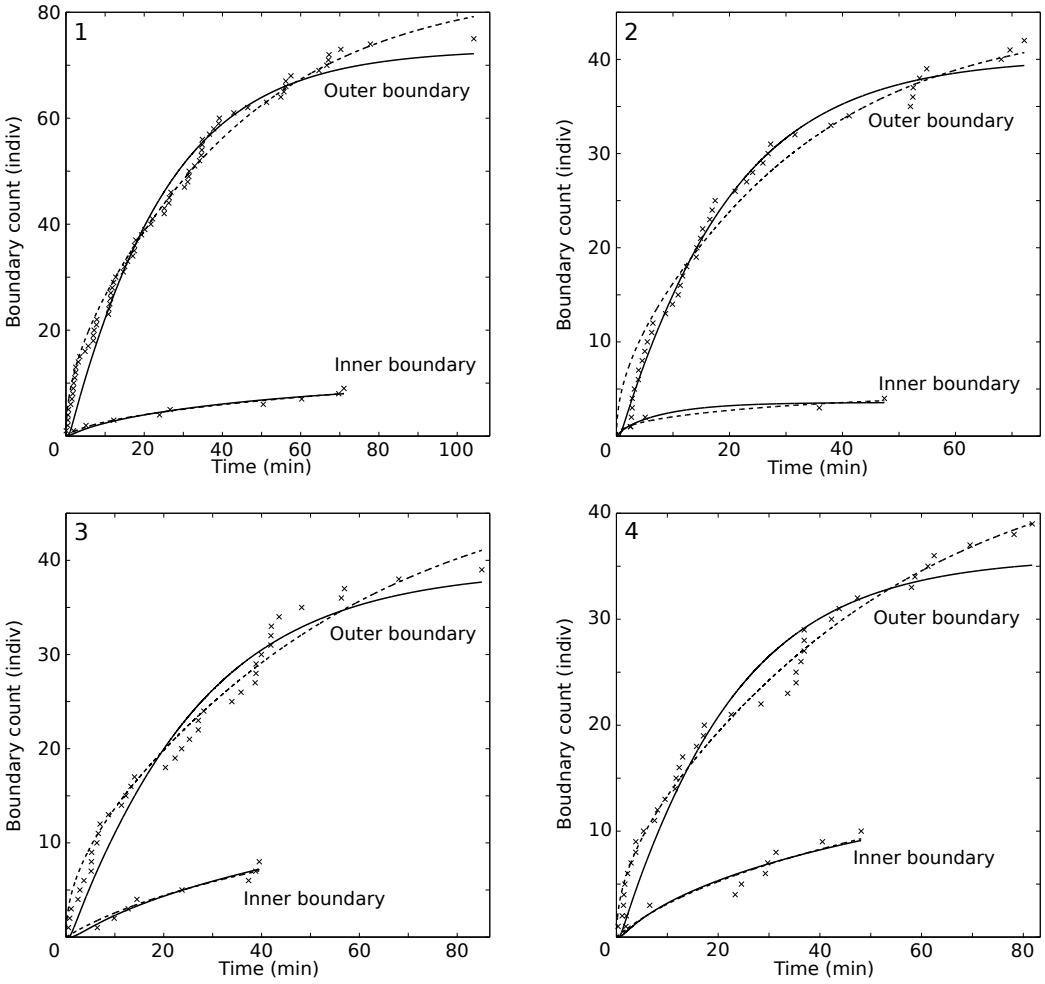

Figure 4: Plots of experimental cumulative boundary count series and fitted curves (using Eq. 15). The number in the top left of each plot indicates the experiment number. Crosses - experimental data, dashed and solid curves - fits using the solution for a reciprocal or stepped reciprocal initial distribution in an annular domain respectively. Inner and outer boundary count series were fitted with different parameters.

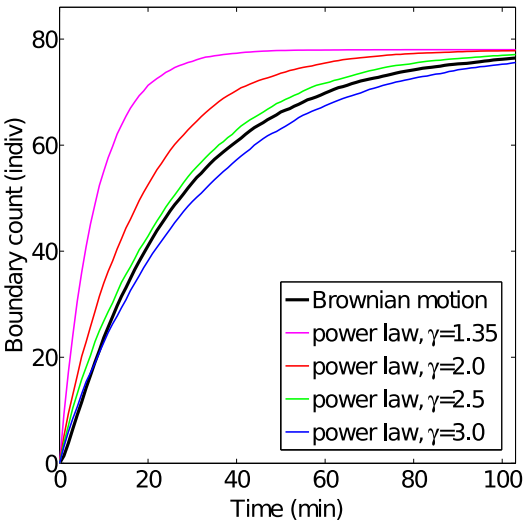

Figure 5: Boundary counts obtained from individual based simulations for different patterns of individual movement. Top to bottom: power law (A.3) with $\gamma = 1.35$ (magenta curve), $\gamma = 2.0$ (red curve), $\gamma = 2.5$ (green curve), Brownian motion (A.2) (thick black curve), power law with $\gamma = 3.5$ (blue curve).

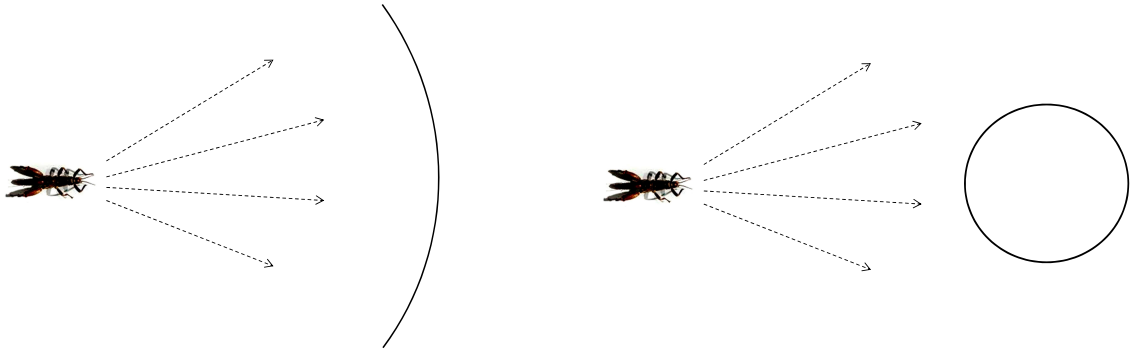

Figure 6: Sketch of the insect movement in the vicinity of a concave (left) and convex (right) edge. For the same range of movement angles, the beetle would cross a boundary of concave shape (left) but would miss a boundary of convex shape (right); further details in the text.